The EMBO Journal Vol.18 No.19 pp.5399–5410, 1999

Functions of the exosome in rRNA, snoRNA and snRNA synthesis

Christine Allmang, Joanna Kufel, Guillaume Chanfreau[1,2], Philip Mitchell, Elisabeth Petfalski and David Tollervey[3]

Institute of Cell and Molecular Biology, University of Edinburgh, Swann Building, King's Buildings, Edinburgh EH9 3JR, UK and [1]GIM-Biotechnologies, Institut Pasteur, 25 rue du Dr Roux, 75724 Paris Cedex 15, France

[2]Present address: Department of Chemistry and Biochemistry, UCLA, Los Angeles CA 90095-1569, USA

[3]Corresponding author
e-mail: d.tollervey@ed.ac.uk

C.Allmang and J.Kufel contributed equally to this work

The yeast nuclear exosome contains multiple 3′→5′ exoribonucleases, raising the question of why so many activities are present in the complex. All components are required during the 3′ processing of the 5.8S rRNA, together with the putative RNA helicase Dob1p/Mtr4p. During this processing three distinct steps can be resolved, and hand-over between different exonucleases appears to occur at least twice. 3′ processing of snoRNAs (small nucleolar RNAs) that are excised from polycistronic precursors or from mRNA introns is also a multi-step process that involves the exosome, with final trimming specifically dependent on the Rrp6p component. The spliceosomal U4 snRNA (small nuclear RNA) is synthesized from a 3′ extended precursor that is cleaved by Rnt1p at sites 135 and 169 nt downstream of the mature 3′ end. This cleavage is followed by 3′→5′ processing of the pre-snRNA involving the exosome complex and Dob1p. The exosome, together with Rnt1p, also participates in the 3′ processing of the U1 and U5 snRNAs. We conclude that the exosome is involved in the processing of many RNA substrates and that different components can have distinct functions.

Keywords: pre-rRNA/RNA processing/*Saccharomyces cerevisiae*/snoRNA/snRNA

Introduction

Eukaryotic cells contain a large number of stable RNA species, nearly all of which are synthesized by post-transcriptional processing from larger precursors. This has long been known for the highly abundant cytoplasmic RNAs, tRNAs and rRNAs, but more recently it has become clear that this is also the case for the small nuclear RNAs (snRNAs), which participate in pre-mRNA splicing, and the small nucleolar RNAs (snoRNAs), which participate in rRNA processing and modification.

Analyses of 3′ processing of the 5.8S rRNA in *Saccharomyces cerevisiae* led to the identification of the exosome complex of 3′→5′ exonucleases (Mitchell *et al.*, 1996, 1997; Allmang *et al.*, 1999). Originally reported to contain five different 3′→5′ exonucleases, it is now likely that the exosome contains at least 10 exonucleases (Allmang *et al.*, 1999). These include six homologues of *Escherichia coli* RNase PH (Rrp41p, Rrp42p, Rrp43p, Rrp45p, Rrp46p and Mtr3p), a homologue of *E.coli* RNase R and RNase II (Rrp44p/Dis3p), and a homologue of *E.coli* RNase D (Rrp6p). Two other components, Rrp4p and Rrp40p, are homologous to each other, and Rrp4p has been shown to be a 3′→5′ exonuclease (Mitchell *et al.*, 1997). The remaining component is Csl4p, which has not been reported to have nuclease activity but does contain a potential S1 RNA binding domain (S.Mian, personal communication), indicating that it is also likely to bind RNA directly. All components of the exosome are essential for viability (Mitchell *et al.*, 1996, 1997; Noguchi *et al.*, 1996; Baker *et al.*, 1998; Allmang *et al.*, 1999) with the exception of Rrp6p, the absence of which results in temperature-sensitive (ts) lethality and impaired growth at all temperatures (Briggs *et al.*, 1998). Normal processing of the 7S pre-rRNA to the mature 5.8S rRNA requires all components of the exosome, but the phenotype of the *rrp6*-Δ strain differs substantially from that of the other mutants, making it unclear whether these function in the same or parallel pathways. In addition to the components of the exosome, the yeast genome contains at least six other open reading frames that are predicted to encode 3′→5′ exonucleases, based on sequence comparisons with *E.coli* enzymes (Mian, 1997; Moser *et al.*, 1997).

5′ processing of the 5.8S rRNA requires the activity of two homologous 5′→3′ exonucleases, Rat1p and Xrn1p, with the major role probably being played by Rat1p (Henry *et al.*, 1994). The same exonucleases are required for the 5′ processing of several snoRNA species, many of which are either synthesized from polycistronic pre-snoRNA transcripts, or are excised from the introns of pre-mRNAs following intron lariat debranching (Ooi *et al.*, 1998; Petfalski *et al.*, 1998). All characterized yeast polycistronic snoRNAs are initially processed by endonuclease cleavage by Rnt1p (Chanfreau *et al.*, 1998a,b; Qu *et al.*, 1999), the yeast homologue of *E.coli* RNase III (Abou Elela *et al.*, 1996), which separates the individual pre-snoRNAs. Rnt1p also processes the pre-rRNA in the 3′ external transcribed spacer (3′-ETS) (Abou Elela *et al.*, 1996; Kufel *et al.*, 1999) and cleaves 3′ extended precursors to the U1, U2 and U5 snRNAs (Chanfreau *et al.*, 1997; Abou Elela and Ares, 1998; Seipelt *et al.*, 1999). In the absence of Rnt1p cleavage, polyadenylated forms of U1 and U2 are synthesized (Abou Elela and Ares, 1998; Seipelt *et al.*, 1999). In *rnt1*-Δ strains the processing of the 3′-ETS and polycistronic pre-snoRNAs is almost completely inhibited, with severe effects on rRNA and snoRNA synthesis. However, 3′ processing of the snRNAs

continues, indicating the existence of alternative processing pathways or activities. The existence of alternative 3′ processing pathways has also been shown for yeast tRNAs (Yoo and Wolin, 1997) and multiple activities can carry out 3′ processing of many small RNAs in *E.coli* (see Li *et al.*, 1998 and references therein).

Here, we investigate the roles of the different exosome components in the 3′ processing of the 5.8S rRNA and pre-rRNA spacer degradation, and present data indicating that the exosome also participates in the 3′ processing of many snRNA and snoRNA species.

Results

The pathway of 5.8S 3′ processing

Three different 3′ extended forms of the 5.8S rRNA can be detected in wild-type strains of yeast. The 7S pre-rRNAs are 3′ extended by ~134 nt to site C_2 in ITS2 (Veldman *et al.*, 1981), while the 6S pre-rRNAs represent 5.8S species with short, probably heterogeneous, 3′ extensions of ~8 nt (Mitchell *et al.*, 1996) (see Figure 1 for a schematic showing the pre-rRNA and processing sites). In addition, the 5.8S + 30 species (Briggs *et al.*, 1998) can be detected at low levels in the wild type (Figure 1D). The 5′ end of the 5.8S rRNA is heterogeneous, with two major forms that differ by 8 nt, designated $5.8S_L$ and $5.8S_S$ (Henry *et al.*, 1994). Since 5′ processing of the 5.8S rRNA precedes 3′ processing, the 7S pre-rRNA, 6S pre-rRNA and 5.8S + 30 species all show long and short forms, e.g. 5.8S + 30_L and 5.8S + 30_S (Figure 1A and D).

Processing of the 5.8S rRNA was compared in strains carrying conditional mutations for the 10 essential components of the exosome, using the ts-lethal *mtr3-1* allele and *GAL*-regulated constructs allowing depletion of Rrp4p, Rrp40p, Rrp41p, Rrp42p, Rrp43p, Rrp44p, Rrp45p, Rrp46p or Csl4p (Figure 1A). As previously reported (Mitchell *et al.*, 1997; Allmang *et al.*, 1999), similar 3′ extended intermediates were observed in each case, forming a ladder up to the position of the 7S pre-rRNAs. The *GAL::rrp41* strain underexpresses Rrp41p in permissive, RSG medium, and therefore shows some accumulation of the extended species in the 0 h sample. Strong accumulation of the 6S pre-rRNA was seen in the strains depleted of Rrp40p or Rrp45p, while 6S was reduced in the Rrp41p-, Rrp44p- or Rrp46p-depleted and mtr3-1 strains and little altered in strains depleted of Rrp4p or Csl4p. Moreover, in strains depleted of Rrp41p, Rrp42p or Rrp43p the position of the 6S pre-rRNA appeared to be displaced up the gel, corresponding to an increase in size of ~3 nt. We conclude that different components of the exosome do not play identical roles in processing of the 6S pre-rRNA.

In *rrp6*-Δ strains, a distinctly different pattern of processing was observed (Figure 1A and D) (Briggs *et al.*, 1998) with accumulation of high levels of the 5.8S + 30 pre-rRNAs. To determine whether Rrp6p and the other exosome components act on the same pre-rRNA processing pathway or function in independent parallel pathways, double-mutant strains were constructed carrying the *rrp6*-Δ allele and either the *GAL::rrp41* (Mitchell *et al.*, 1997) or the *GAL::rrp45* allele. Depletion of either Rrp41p or Rrp45p from a strain lacking Rrp6p led to the progressive loss of the 5.8S + 30 processing intermediate, clearly

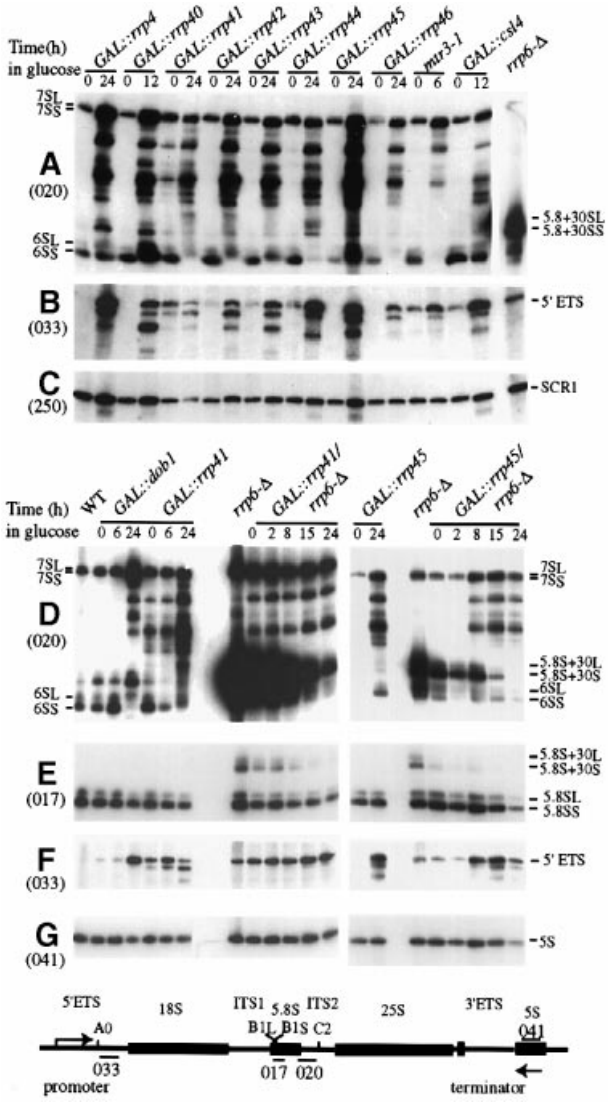

Fig. 1. Northern analysis of processing of the 5.8S rRNA and degradation of the 5′ ETS region of the pre-rRNA in exosome mutants. (**A** and **D**) Hybridization with probe 020, complementary to the 5.8S–ITS-2 boundary. (**B** and **F**) Hybridization with probe 033, complementary to the 5′-ETS region around + 270. (**E**) Hybridization with probe 017, complementary to the 5′ region of the mature 5.8S rRNA. (**C**) Hybridization with probe 250, complementary to SCR1 RNA. (**G**) Hybridization with probe 041, complementary to the mature 5S rRNA. Probe names are indicated in parentheses on the left. RNA was extracted from strains carrying *GAL*-regulated constructs following transfer from permissive, RSG medium to repressive, glucose medium for the times indicated. The *mtr3-1* strain was grown in glucose medium at 25°C or transferred to 37°C for 6 h. The *rrp6*-Δ strain was grown on glucose medium at 30°C.

showing that Rrp41p and Rrp45p act epistatically to Rrp6p in the 5.8S processing pathway (Figure 1D). Metabolic labelling of an *rrp6*-Δ strain also indicated that Rrp6p participates in the major 5.8S rRNA processing pathway (Briggs *et al.*, 1998).

Mutations in the putative ATP-dependent RNA helicase Dob1p (Mtr4p) also interfere with 3′ processing of the 5.8S rRNA (de la Cruz *et al.*, 1998). A *GAL::dob1* strain genetically depleted of Dob1p accumulated both the 5.8S + 30 species and larger intermediates that are seen in other exosome mutants (Figure 1D). The 6S pre-rRNAs accumulated in the *GAL::dob1* strain 2 and 6 h after

transfer to glucose medium but were reduced after 24 h. This probably occurred because processing of the pre-rRNA is strongly inhibited prior to synthesis of 6S, as shown by the high accumulation of the 7S and 5.8S + 30 pre-rRNAs.

Strains depleted of exosome components or Dob1p, or carrying the *mtr3-1* or *rrp6*-Δ mutations, accumulated the excised 5′ ETS region and degradation intermediates (Figure 1B and F) (de la Cruz *et al.*, 1998; Allmang *et al.*, 1999). The levels of the degradation intermediates were quite variable among the exosome mutants. This indicates that, while degradation of the 5′ ETS involves the entire exosome complex, different components do not have identical functions during this activity.

Pre-snoRNA processing

Many yeast snoRNAs are synthesized by post-transcriptional processing, either from the excised introns of pre-mRNAs or from polycistronic transcripts that include multiple snoRNAs. In higher eukaryotes, both 5′ and 3′ processing of pre-snoRNAs involves exonuclease activities (Caffarelli *et al.*, 1994, 1996; Cecconi *et al.*, 1995; Cavaillé and Bachellerie, 1996; Kiss *et al.*, 1996). 5′ processing of several yeast pre-snoRNAs was shown to require the 5′→3′ exonucleases Rat1p and Xrn1p, with the major role being performed by Rat1p (Larimer *et al.*, 1992; Kenna *et al.*, 1993; Petfalski *et al.*, 1998; Villa *et al.*, 1998). Northern analysis of RNA extracted from the *rrp6*-Δ strain showed many species with a discrete shift in gel mobility that would correspond to an increase in length of 3 nt (Figure 2A). This was observed for the intronic snoRNAs U18, U24 and snR39, as well as U14 and snR41, which are encoded in dicistronic and polycistronic transcripts, respectively (Figure 2A). In contrast, the gel mobilities of snoRNAs that are transcribed from their own promoter and terminator, snR10 (Figure 2A) and U3 (data not shown), were unaffected by deletion of *RRP6*. The dicistronic snoRNA, snR190, which is cotranscribed with U14, was also not affected (Figure 2A).

Primer extension revealed that the position of the 5′ end was unaffected for each of these snoRNAs (Figure 2B) indicating that the altered gel mobility represents a failure in the 3′ trimming of the snoRNA. For U24 the presence of a 3′ extension was confirmed by RNase protection (data not shown).

Strains individually depleted for each of the other exosome components or Dob1p, or carrying the *rrp4-1*, *mtr3-1* or *dob1-1* mutations at non-permissive temperature, were analysed for processing of U14, U18, U24 and snR190 (shown for *GAL::rrp41* and *GAL::rrp45* in Figure 2C and *dob1-1* in Figure 2A). No clear alteration in the length of the mature snoRNAs was observed, showing that depletion or mutation of other individual components of the exosome or Dob1p does not inhibit snoRNA 3′ end trimming. Double-mutant strains lacking Rrp6p and depleted of either Rrp41p or Rrp45p were also analysed (shown for *GAL::rrp41*/*rrp6*-Δ in Figure 3I). The length of the 'almost-mature' snoRNAs in these strains was the same as in strains lacking only Rrp6p. We conclude that 3′ trimming of the snoRNAs requires specifically the Rrp6p component of the exosome complex. In addition, longer extended forms were observed for U14, U18 and U24, but not for snR190 (Figure 3 and data not shown).

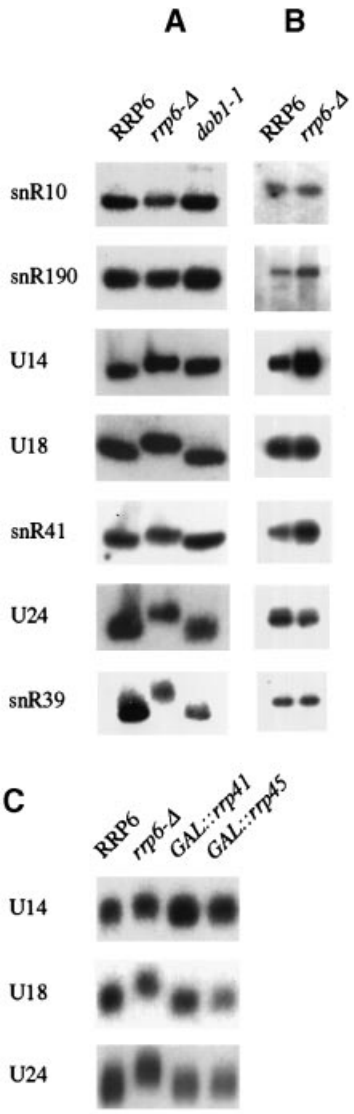

Fig. 2. Deletion of *RRP6* inhibits 3′ trimming of pre-snoRNAs. (**A** and **C**) Northern hybridization of snoRNAs. (**B**) Primer extension on snoRNAs. RNA was extracted from the *RRP6* and *rrp6*-Δ strains following growth at 30°C, from the *dob1-1* strain 6 h after transfer to 37°C and from the *GAL::rrp41* and *GAL::rrp45* strains following growth for 24 h on glucose medium. The gel migration shown for snR10 and snR190 in (A) is longer than that shown for the other, smaller RNA species to confirm that these were not extended in the *rrp6*-Δ strain.

Yeast U18 and U24 are intron encoded (Maxwell and Fournier, 1995; Qu *et al.*, 1995; Kiss-László *et al.*, 1996) and are synthesized predominantly from the debranched intron lariats (Ooi *et al.*, 1998; Petfalski *et al.*, 1998). As previously reported (Petfalski *et al.*, 1998), the species corresponding to the introns that are 3′ unprocessed but 5′ processed to the end of the mature snoRNAs [U18-3′ (253 nt) and U24-3′ (192 nt)] are detected in the wild-type strain (Figure 3IIB and IIC, lanes 1, 3, 5 and 7). Both U24-3′ and U18-3′ can be detected on Northern blots with probes that hybridize specifically with 3′ extended species (Figure 3II, lanes 7 and 8) and both are lost in strains carrying mutations in the 5′→3′ exonucleases Rat1p and Xrn1p (Petfalski *et al.*, 1998). In strains lacking Rrp6p, the level of U24-3′ was increased and ladders of intermediates appeared both below and above

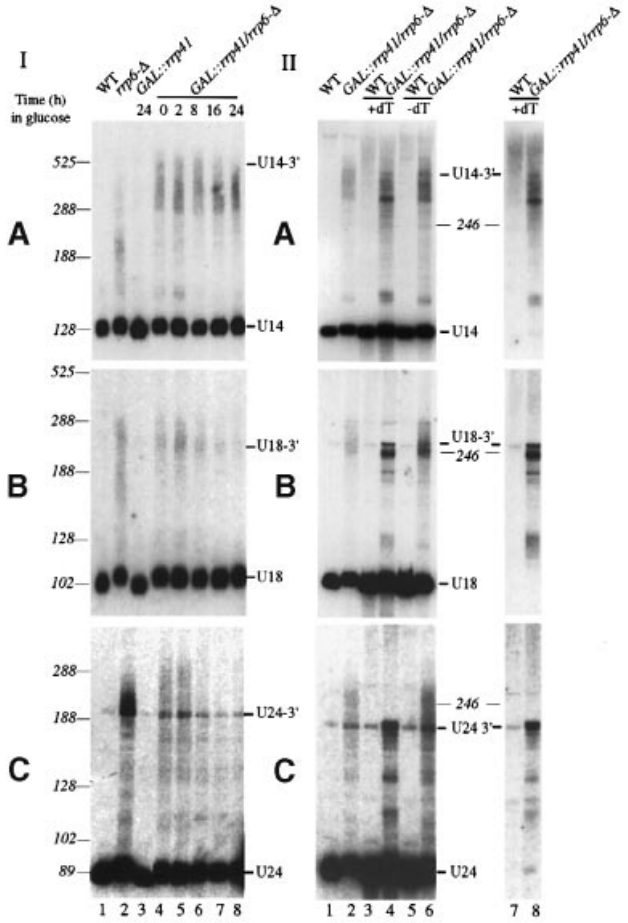

Fig. 3. Long 3′ extended forms of snoRNAs accumulate in exosome mutants. (**I** and **II**) Northern hybridization with probes directed against (**A**) mature U14 (202); (**B**) mature U18 (215); (**C**) mature U24 (204). RNA was extracted from the *RRP6* and *rrp6*-Δ strains following growth at 30°C, from the *GAL::rrp41* strain following growth for 24 h on glucose medium and from the *GAL::rrp41*/*rrp6*-Δ strain following transfer from RSG medium (0 h) to glucose medium for the times indicated. The positions of migration of SCR1 (525 nt), 7S pre-rRNA (288 nt), snR10 (246 nt) and 5.8S + 30 pre-rRNA (188 nt) determined by hybridization of the same filters are indicated as size markers. Mature U18 is 102 nt, U24 is 89 nt and U14 is 126 nt. (II) RNase H treatment of RNA samples. Lanes 1 and 2, untreated samples; lanes 3 and 4, samples treated with RNase H and oligo(dT); lanes 5 and 6, samples treated with RNase H in the absence of added oligo(dT); lanes 7 and 8, the samples shown in lanes 3 and 4 were rehybridized with probes across the ends of the mature snoRNAs that hybridize specifically with 3′ extended species (210, 206, 213). RNA from the wild type (WT) and *GAL::rrp41rrp6*-Δ 2 h samples shown in (I) was used.

this species (Figure 3IC, lane 2). To test the possibility that the species observed above U24-3′ correspond to polyadenylated forms, RNA from the wild-type and the *GAL::rrp41*/*rrp6*-Δ strain 2 h after transfer to glucose medium was deadenylated *in vitro* with oligo(dT) and RNase H. On deadenylation the heterogeneous species observed above the U24-3′ band were lost and the U24-3′ signal was increased (Figure 3IIC, compare lanes 4 and 6). Strains depleted of Rrp41p (Figure 3IC, lane 3) did not clearly accumulate U24-3′, whereas accumulation of U24-3′ and a ladder of smaller intermediates were detected on depletion of Rrp45p and in a *rrp4-1* strain (data not shown), demonstrating that processing of U24-3′ is not specific for Rrp6p. Extended forms of U24-3′

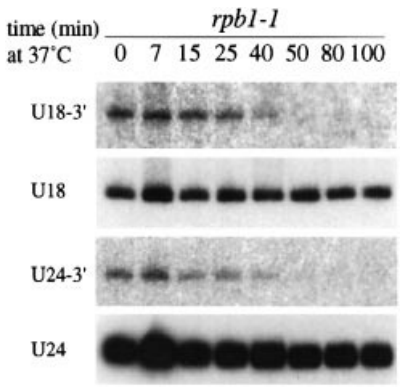

Fig. 4. Transcriptional inhibition leads to the loss of the 3′ extended snoRNA species. RNA was extracted from the *rpb1-1* strain pre-grown at 23°C following transfer to 37°C for the times indicated. Northern hybridization was performed with oligonucleotide probes directed against mature U18 (205), mature U24 (214), U18-3′ (206) and U24-3′ (213).

were not observed in these strains, and the formation of polyadenylated species may be specific for *rrp6*-Δ. It is notable that *RRP6* was originally identified as a mutation that suppressed a defect in polyadenylation (Briggs *et al.*, 1998).

For U18, heterogeneous 3′ extended species were observed in the *rrp6*-Δ strain, and these were longer and more discrete in the *GAL::rrp41*/*rrp6*-Δ double mutant (Figure 3IB). These were estimated to be in the range 250–300 nt. Following deadenylation, the U18-3′ RNA is clearly seen to be strongly accumulated in the *GAL::rrp41*/*rrp6*-Δ strain, with a ladder of intermediates extending up to this position (Figure 3IIB, lanes 4 and 8). The same species are detected in the non-deadenylated sample (Figure 3IIB, lane 6), but are less clear.

snR190 and U14 are cotranscribed, separated by Rnt1p cleavage and then 5′ processed by Rat1p (Zagorski *et al.*, 1988; Chanfreau *et al.*, 1998b; Petfalski *et al.*, 1998). Extended forms of U14 were observed in *rrp6*-Δ strains but were both more abundant and longer in *GAL::rrp41*/*rrp6*-Δ strains that were also depleted of Rrp41p (Figure 3A). On deadenylation these species formed a ladder up to the U14-3′ RNA, which was estimated to be ~525 nt in length. It seems probable that U14-3′ extends to the transcription termination site, which has not yet been located. Extended snoRNAs were not observed in strains depleted of Dob1p (data not shown).

To determine whether U18-3′ and U24-3′ species are processing intermediates or dead-end products, a transcription inhibition experiment was performed (Figure 4). RNA was recovered from a *rbp1-1* strain, carrying a ts mutation in RNA polymerase II, at time points after shift to the non-permissive temperature. Following transcription inhibition, U18-3′ and U24-3′ were progressively lost, indicating that they are normal processing intermediates.

We conclude that the exosome participates in the 3′ processing of snoRNAs, processing the primary transcript of the dicistronic snR190-U14 snoRNAs and the debranched intron lariats containing the U18 and U24 snoRNAs. As seen for 5.8S synthesis, snoRNA processing is at least biphasic. Initial processing is partially inhibited, but not blocked, by different mutations in the exosome, whereas trimming of the final 3 nt specifically requires

Rrp6p. The additive effect of the *rrp41* and *rrp6* mutations on U18 and U14 synthesis is, however, in contrast to the epistatic interactions observed for 5.8S processing. In the absence of Rrp6p some polyadenylation of processing intermediates also occurs.

snRNA synthesis

Since a number of snRNAs have been shown to undergo 3′ processing we analysed snRNA species for alterations in exosome mutants.

Analysis of the U4 snRNA showed the existence of low levels of two longer forms (U4-3′I and U4-3′II) in the wild type (Figure 5, lanes 1 and 12). Both species were detected with either the internal U4 probe (oligo 243) (Figure 5B) or a probe complementary to the sequence across the 3′ end of the mature U4 (oligo 246), which hybridizes only to 3′ extended species (Figure 5A). U4-3′I is a set of heterogeneous species carrying short 3′ extensions similar in length to those detected in the 6S pre-rRNA. Oligo 246 detects only the longer forms of U4-3′I. The U4-3′II species is ~140 nt larger than mature U4 and is presumably a normal processing intermediate since it is detected in wild-type cells. In strains depleted of the exosome components Rrp41p (Figure 5, lanes 2 and 3) or Rrp45p (Figure 5, lanes 7 and 8), or lacking Rrp6p (Figure 5, lane 15), the levels of U4-3′I and U4-3′II were increased and a ladder of intermediates was observed that extended from the size of U4-3′I to that of U4-3′II. The *GAL::rrp41* strain shows some accumulation of the extended species in the 0 h sample due to under-expression of Rrp41p (Figure 5, lane 2). The same species were accumulated in a strain depleted of Dob1p (data not shown). The accumulation of these intermediates was not stronger in the *rrp6*-Δ strain that was also depleted of Rrp41p or Rrp45p than in the *rrp6*-Δ single-mutant strain (data not shown). In strains lacking Rnt1p, U4-3′II RNA was absent whilst the levels of the U4-3′I species were increased. These observations suggested that the U4-3′II is generated by Rnt1p cleavage and acts as an entry site for the exosome complex.

Strains lacking Rnt1p also accumulated longer 3′ extended forms of U4 (Figure 5, lanes 13 and 14; 4-fold more RNA was loaded in lane 14 to allow visualization of the longer 3′ extended species). These were more abundant in *rnt1*-Δ strains that were also depleted of Rrp41p (Figure 5, lanes 4–6), Rrp45p (Figure 5, lanes 9–11) or Rrp6p (Figure 5, lane 16). Particularly in the *rnt1*-Δ/*rrp6*-Δ strain (Figure 5B, lane 16) these were seen to extend to a distinct species (U4-3′III) of ~590 nt. It seems likely that these represent intermediates in the 3′ processing of U4 from U4-3′III, which most probably extends to the transcription termination site. Little effect on the 3′ extended forms of U4 was seen on treatment with RNase H and oligo(dT) (data not shown).

Rnt1p cleaves on both sides of extended, imperfect stems with closing AGNN tetraloops (Chanfreau *et al.*, 1998a). Inspection of the U4 3′ flanking region identified good consensus Rnt1p cleavage sites (Figure 6D). To determine whether this represented a genuine substrate for Rnt1p, cleavage was assayed *in vitro*. The region of the U4 3′ flanking sequence from positions +49 to +235, which includes the putative cleavage sites, was transcribed *in vitro* (see Materials and methods). The sites cleaved

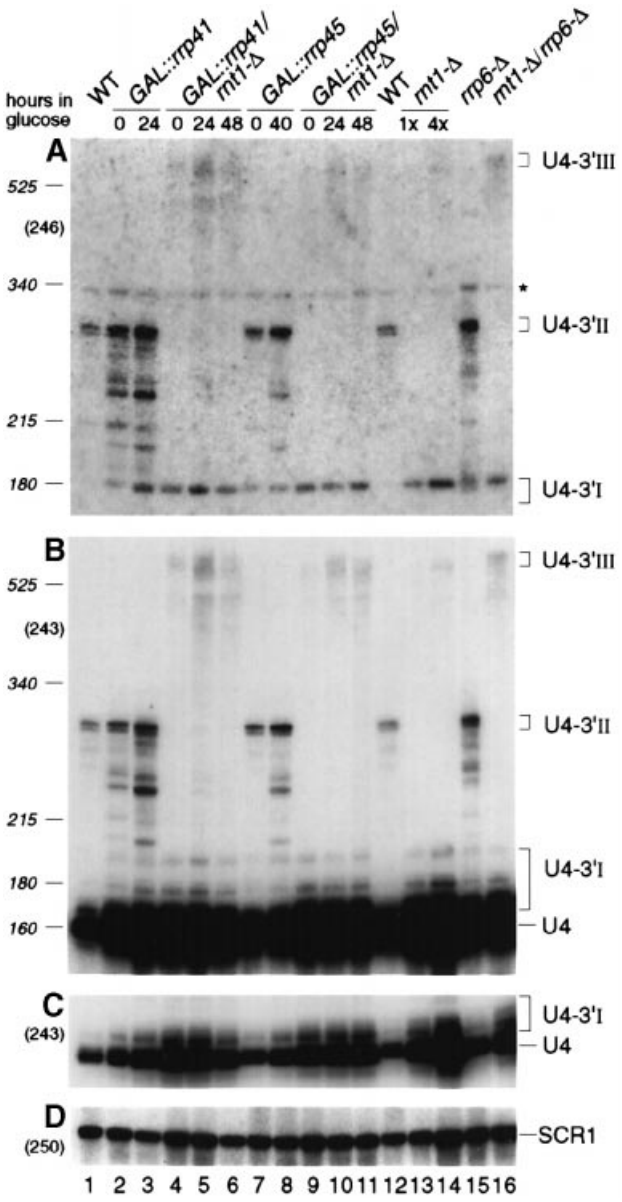

Fig. 5. Northern analysis of processing of U4 snRNA in *rnt1*-Δ and exosome mutants. RNA was extracted from strains carrying *GAL*-regulated constructs following transfer from permissive, RSG medium to repressive, glucose medium at 30°C for the times indicated, or from the wild-type (WT), *rnt1*-Δ and *rrp6*-Δ strains grown on glucose medium at 30°C. RNA was separated on a 6% polyacrylamide gel and hybridized with oligonucleotide probes. (**A**) Oligo 246 complementary to the region across the 3′ end of the mature U4 snRNA. (**B** and **C**) Oligo 243 complementary to the mature U4 snRNA. (**D**) Oligo 250 complementary to the mature SCR1 RNA; the panels show successive hybridizations of the same filter. Probe names are indicated in parentheses on the left and the positions of detected RNA species are indicated on the right. (C) presents a weaker exposure of the same gel as (B). (C and D) present only relevant regions of the Northern blots. The species marked with * in (A) probably results from a cross-hybridization with another RNA since it was not detected in (B). The amount of total RNA loaded in lane 14 is 4-fold higher than in lane 13 and other lanes. The positions of migration of SCR1 (525 nt), MRP RNA (340 nt), $U5_L$ (215 nt) and $U5_S$ (180 nt) determined by hybridization of the same filter are indicated as size markers. Mature U4 is 160 nt.

in vitro by recombinant His_6–Rnt1p were identified by primer extension with oligo 249 (Figure 6A). Two major stops, corresponding to sites of cleavage between

nucleotides +135/+136 (site I in Figure 6D) and +169/+170 (site II in Figure 6D) with respect to the 3′ end of the mature U4, were detected following incubation with His_6–Rnt1p (Figure 6A, lane 5); these sites were not detected in the no-enzyme controls (Figure 6A, lane 6). The sites lie on both sides of the predicted stem–loop structure and are in good agreement with the consensus for other Rnt1p cleavage sites (Figure 6D). Additional minor stops were detected one nucleotide 5′, corresponding to positions +134/+135 and +168/+169 (smaller arrows in Figure 6D). To confirm that these stops represented sites of endonuclease cleavage, internally labelled RNA transcripts (Figure 6B) were also assayed using either recombinant His_6–Rnt1p or extracts prepared from *RNT1*$^+$ and *rnt1*-Δ strains of yeast (see Materials and methods). Incubation with either recombinant Rnt1p (Figure 6B, lanes 3–6) or the yeast extract containing Rnt1p (Figure 6B, lane 7), resulted in the appearance of discrete cleavage products that were not observed in the input RNA (Figure 6B, lane 2) or with the yeast extract lacking Rnt1p (Figure 6B, lane 8). The estimated sizes of these products are in good agreement with the predicted sizes of the products of cleavage at both sites I and II (Figure 6B; the predicted locations and sizes of the cleavage products are indicated below the gel).

To identify the position of *in vivo* processing, we performed primer extension using an oligo that hybridizes to the U4 flanking sequence 3′ to the Rnt1p cleavage site (oligo 249). In the wild-type strain, a primer extension stop was detected between nucleotides +135 and +136, precisely matching *in vitro* cleavage site I (Figure 6C, lane 1). This stop was absent from the *rnt1*-Δ strain (Figure 6C, lane 2). *In vivo* cleavage could not be detected at site II, but the primer gave a high background in this region (data not shown). Following cleavage of the pre-rRNA in the 3′-ETS by Rnt1p, the excised 3′ fragment is degraded 5′→3′ by Rat1p (Kufel *et al.*, 1999). The primer extension stop observed in the *rat1-1* strain at position +135/+136 was stronger than in the wild type, supporting the conclusion that this is a site of *in vivo* endonuclease cleavage (Figure 6C, lane 3).

We conclude that Rnt1p cleaves the 3′ flanking sequence of the U4 snRNA. The predominant *in vivo* cleavage is at position +135/+136, generating the U4-3′II RNA. Cleavage may also occur at +169/+170, although no species corresponding to this cleavage was detected by Northern hybridization. The +135/+136 cleavage acts as a site of entry for the exosome complex. Since U4-3′II is detected in wild-type cells it is presumably a normal processing intermediate. In the absence of Rnt1p, longer transcripts are detected; these are also substrates for the exosome since they accumulate at higher levels in double-mutant strains, but can be efficiently processed to mature U4 by another pathway(s). It seems likely that the accumu-

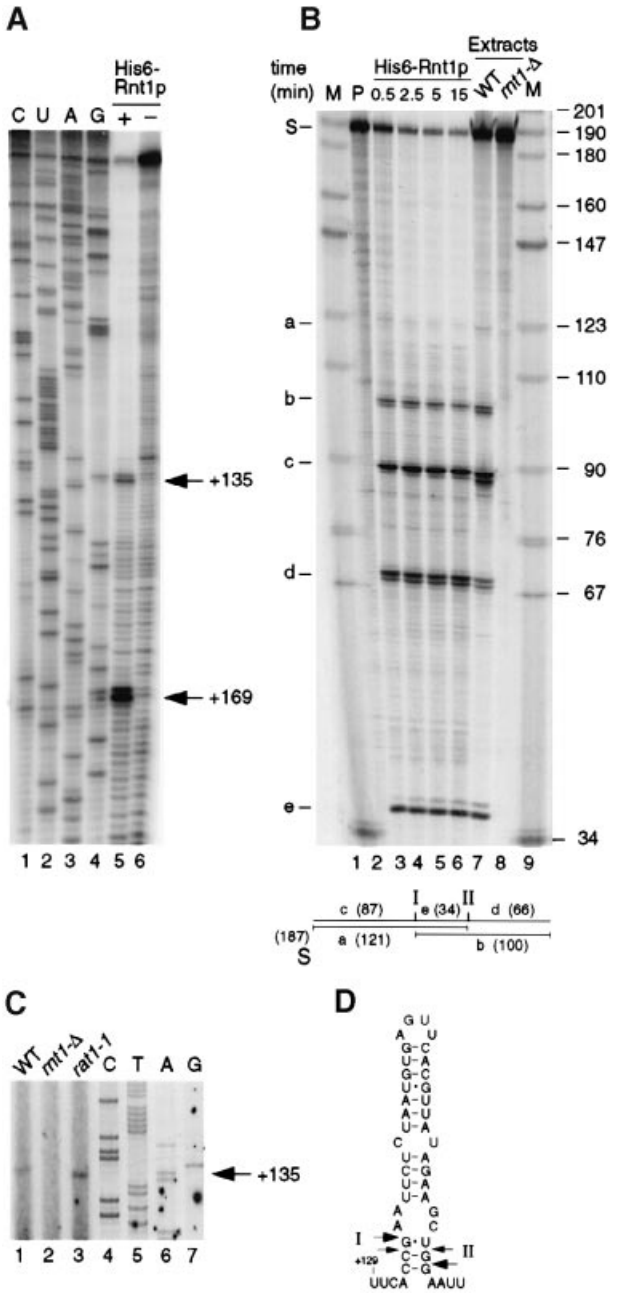

Fig. 6. Rnt1p cleaves the 3′ end of the U4 precursor. (**A**) Mapping of the *in vitro* Rnt1p cleavage sites. Primer extension was performed using oligo 249 on the model U4-3′ RNA incubated with buffer (lane 6) or recombinant His_6–Rnt1p (lane 5) as described in Materials and methods. DNA sequencing reaction on a PCR product encompassing the region of the 3′ end of U4 from position +49 to +235, using the same primer, was run in parallel (lanes 1–4). The primer extension stops at positions +135 and +169 are indicated. (**B**) *In vitro* cleavage of an internally labelled model U4-3′ RNA substrate by Rnt1p. ^{32}P-labelled U4-3′ RNA was incubated at 23°C in the following conditions: lane 2, Rnt1p buffer; lanes 3–6, Rnt1p buffer with 20 ng of recombinant His_6–Rnt1p for the times indicated; lane 7, with whole-cell extract from a wild-type (WT) strain of yeast; lane 8, with whole-cell extract from a *rnt1*-Δ strain; lanes 1 and 9, RNA size markers. The positions of DNA size markers are indicated on the right of the gel. The cleavage products obtained are labelled a–e on the left and the predicted origin of each species is indicated below the gel. S: substrate, 187 nt; a: 5′ end of transcript to site II, 121 nt; b: 3′ end of transcript to site I, 100 nt; c: 5′ end of transcript to site I, 87 nt; d: 3′ end of transcript to site II, 66 nt; e: site I to site II, 34 nt. (**C**) Mapping of the Rnt1p 5′ cleavage site *in vivo*. Primer extension analysis through the 3′ end of the pre-U4 was performed using primer 249 hybridizing downstream of position + 212. RNA was extracted from wild-type (WT, lane 1) and *rnt1*-Δ (lane 2) strains grown at 30°C and from a *rat1-1* strain following transfer to 37°C for 2 h (lane 3). DNA sequencing reactions were run in parallel (lanes 4–7). The primer extension stop at position +135 is indicated. (**D**) Computer-predicted RNA structure in the U4 3′ flanking region that contains the Rnt1p cleavage sites. The major cleavage sites I (between nucleotides 135 and 136) and II (between nucleotides 169 and 170) are indicated by arrows.

Table I. Phosphoimager quantitation of Northern hybridization data from Figures 5 and 7

	WT	*GAL::rrp41* (24 h)	*GAL::rrp45* (40 h)	*rrp6*-Δ	*rnt1*-Δ
$U5_L$	1.27	1.63	0.63	1.9	0.025
$U5_S$	1	13.5	6.1	4.5	9.4
$U5_S/U5_L$	0.79	8.28	9.68	2.37	376
U4	1	3.8	2.9	2.5	6.5
SCR1	1	1.05	1.27	1.59	1.46

$U5_L$ and $U5_S$ levels are expressed relative to the signal for $U5_S$ in the wild-type strains.

lation of the short 3′-extended U4-3′I species is not a direct product of inhibition of the exosome complex, but is associated with the activation of an alternative processing pathway, since these species are increased relative to the wild type in strains lacking either exosome components or Rnt1p.

Quantitation of the Northern data (Table I) revealed that the mature U4 accumulates above the wild-type level in both the exosome and Rnt1p mutant strains relative to the cytoplasmic 7SL RNA homologue SCR1 (Table I and Figure 5D) or the nucleolar MRP RNA (data not shown). We conclude that a significant fraction of the U4 or pre-U4 population is normally degraded by an exosome-dependent pathway in wild-type strains.

Two forms of the U5 snRNA, $U5_L$ and $U5_S$, which differ at their 3′ ends, are observed in wild-type yeast strains (Patterson and Guthrie, 1987). Species with short, heterogeneous 3′ extensions were observed for both $U5_L$ ($U5_L$-3′) and $U5_S$ ($U5_S$-3′). These species are detected with an internal U5 probe (oligo 244; Figure 7A and D), and also with probes across the 3′ end of $U5_L$ (oligo 247; Figure 7B) or across the 3′ end of $U5_S$ (oligo 248; Figure 7C), although only the longer forms are detected by oligos 247 and 248. Both $U5_L$-3′ and $U5_S$-3′ were detected at low levels in wild-type strains (Figure 7, lanes 1 and 12). These, and a longer species, U5-3′I, were accumulated in strains depleted of Rrp41p (Figure 7, lanes 2 and 3) or Rrp45p (Figure 7, lanes 7 and 8), or lacking Rrp6p (Figure 7, lane 15) and were mildly accumulated in strains depleted of Dob1p (data not shown). In *rrp6*-Δ strains that were also depleted of Rrp41p, the accumulation of these intermediates was not clearly different from the *rrp6*-Δ single-mutant strains (data not shown). Cleavage sites for Rnt1p are present in the U5 3′ flanking region (Chanfreau *et al.*, 1997). In the absence of Rnt1p, $U5_L$-3′ and U5-3′I were absent and the level of $U5_L$ was strongly reduced (Figure 7D, lanes 13 and 14 and Table I). Based on their gel mobilities, the $U5_L$-3′ species extend up to a position close to the 5′ Rnt1p cleavage site [site λ in Figure 7 and Chanfreau *et al.* (1997)], while the larger U5-3′I species extends to a position close to the 3′ Rnt1p cleavage site [site σ in Figure 7 and Chanfreau *et al.* (1997)]. The accumulation of these species in exosome mutants suggests that the Rnt1p cleavages normally act as entry sites for the exosome. In the absence of Rnt1p (Figure 7A, lanes 13 and 14), longer 3′ extended forms of U5 were detected in a ladder to a species designated U5-3′II of ~690 nt (Figure 7A). These were strongly increased in *rnt1*-Δ strains also depleted of Rrp41p, Rrp45p or Rrp6p (Figure

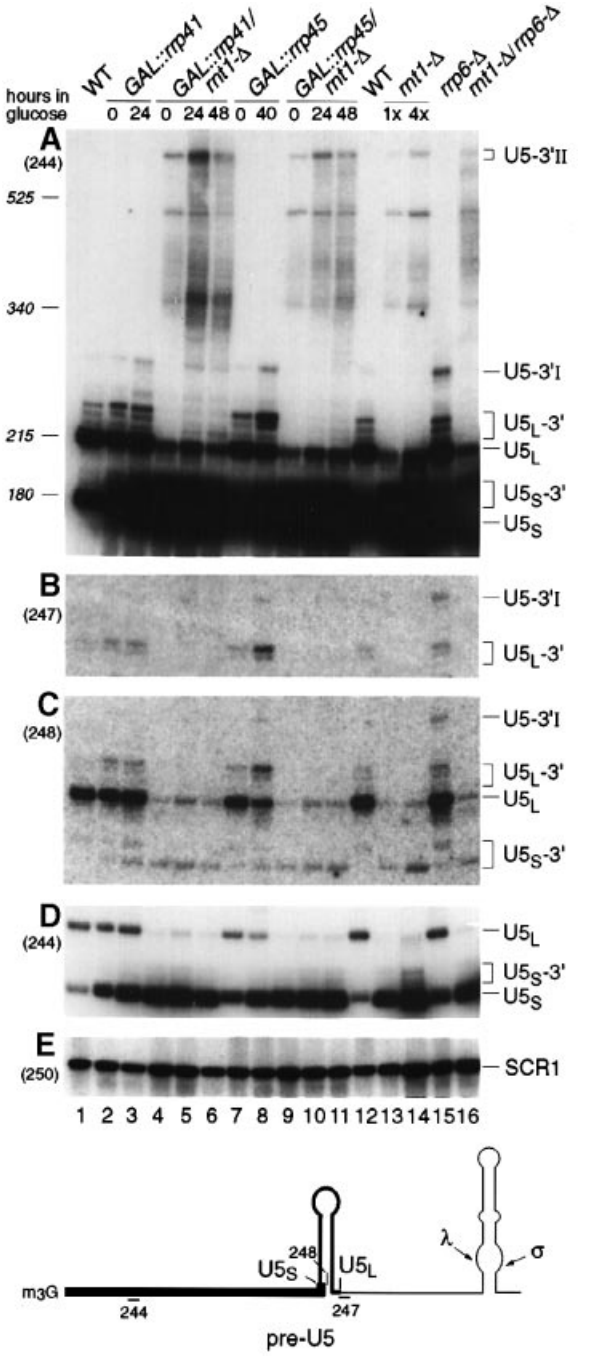

Fig. 7. Northern analysis of processing of U5 snRNA in *rnt1*-Δ and exosome mutants. Strains were grown and RNA was prepared as described for Figure 5. (**A** and **D**) Hybridization with oligo 244 complementary to the mature U5 snRNA. (**B**) Hybridization with oligo 247 complementary to the region across the 3′ end of mature $U5_L$ snRNA. (**C**) Hybridization with oligo 248 complementary to the region across the 3′ end of mature $U5_S$ snRNA. Probe names are indicated in parentheses on the left and the positions of detected RNA species are indicated on the right. (B, C and D) present only relevant regions of the Northern blot. The amount of total RNA loaded in lane 14 is 4-fold greater than in lane 13 and other lanes. (**E**) Oligo 250 complementary to the mature SCR1 RNA; the panels show successive hybridizations of the same filter. The positions of migration of SCR1 (525 nt), MRP RNA (340 nt) determined by hybridization of the same filter are indicated as size markers. Mature $U5_L$ is 215 nt and $U5_S$ is 180 nt.

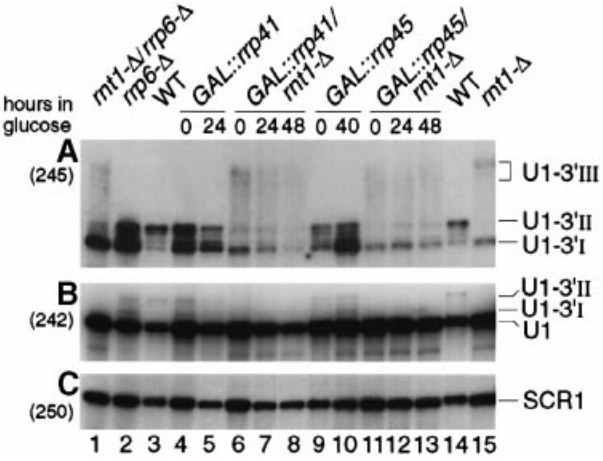

Fig. 8. Northern analysis of processing of U1 snRNA in *rnt1*-Δ and exosome mutants. Strains were grown and RNA was prepared as described for Figure 5. (**A**) Hybridization with oligo 245 complementary to the region across the 3′ end of mature U1 snRNA. (**B**) Hybridization with oligo 242 complementary to the mature U1 snRNA. Probe names are indicated on the left and the positions of RNA species detected are indicated on the right. (**C**) Oligo 250 complementary to the mature SCR1 RNA; the panels show successive hybridizations of the same filter.

7A). It seems likely that U5-3′II extends to the transcription termination site and that the ladder represents intermediates in its 3′ processing to $U5_S$. Little effect on the 3′ extended forms of U5 was seen on treatment with RNase H and oligo(dT) (data not shown).

The signal for $U5_S$ was strikingly increased relative to $U5_L$, SCR1 RNA or MRP RNA (data not shown) in strains depleted of Rrp41p (Figure 7, lanes 2 and 3), Rrp45p (Figure 7, lanes 7 and 8) or Dob1p (data not shown), or lacking Rrp6p (Figure 7, lane 15) or Rnt1p (Figure 7D, lane 13). These results are quantified in Table I; the $U5_S$:$U5_L$ ratio is changed >10-fold on depletion of Rrp41p or Rrp45p and the total amount of $U5_L$ + $U5_S$ synthesized is substantially more than wild type. We conclude that when the normal processing pathway is active, a large fraction of the pre-$U5_S$ or $U5_S$ population is degraded. $U5_S$ is unusual among snRNAs in not having a terminal stem–loop structure beyond the Sm binding site to stabilize the 3′ end, which may make it particularly liable to degradation.

A 3′ extended form of the U1 snRNA that is likely to extend to the Rnt1p cleavage site has been reported for wild-type strains (Seipelt *et al.*, 1999). This presumably corresponds to the species designated U1-3′II that we detect on Northern hybridization (Figure 8, lanes 3 and 14), which is absent in *rnt1*-Δ strains (Figure 8, lane 15). The yeast U1 RNA is 568 nt in length (Kretzner *et al.*, 1987; Siliciano *et al.*, 1987), substantially larger than U4 and U5, and the precursors are therefore less well separated in Figure 8 than in Figures 5 and 7. In addition, we see shorter 3′ extended forms, U1-3′I, which are strongly accumulated in strains depleted of Rrp41p (Figure 8, lanes 4 and 5) or Rrp45p (Figure 8, lanes 9 and 10), or lacking Rrp6p (Figure 8, lane 2). Unlike the longer U1-3′II species, the shorter U1-3′I persists in *rnt1*-Δ strains (Figure 8, lane 15). The *rnt1*-Δ strain accumulates longer, heterogeneous 3′ extended species, U1-3′III, which are reported to be polyadenylated (Seipelt *et al.*, 1999). As for U4 and U5, these long species are more strongly accumulated in *rnt1*-Δ strains that also lack exosome components. In contrast to the results for U4 and U5, the mature U1 is not clearly accumulated above wild-type levels in the exosome mutants.

We conclude that 3′ processing of U1, like U4 and U5, involves 3′ cleavage by Rnt1p and processing by the exosome, although mutations in individual components of the complex do not block processing.

Discussion

The characterization of the exosome complex raised an obvious question: why are so many different exonucleases present in the complex? Possible explanations are that multiple enzymes might function in the processing of single RNA substrates or that different enzymes might be preferentially active on different substrates. We have presented initial evidence for both of these phenomena, as well as identifying a large number of additional substrates for the complex.

During the processing of the 7S pre-rRNA to the 5.8S rRNA, the specificity of the exonuclease appears to change at least twice (see Figure 9A), a phenomenon that we refer to as exonuclease hand-over. Moreover, the effects on the 6S pre-rRNA vary between different mutants, showing that they do not have identical functions. The putative RNA helicase Dob1p/Mtr4p appears to be required for each of these processing steps. The 5.8S + 30 pre-rRNAs extend to the 3′ side of a predicted stable stem–loop structure, which includes the two terminal nucleotides of the mature 5.8S rRNA (Yeh and Lee, 1990). It is, however, unclear whether processing is inhibited by the stem–loop structure itself, or by the consequent very close proximity to the 3′ region of the mature 5.8S rRNA, which is likely to be associated with ribosomal proteins. The simplest interpretation of the data would be that all of the essential exosome components, but not Rrp6p, are required for normal processing of the 7S pre-rRNA to 5.8S + 30. At this point, Rrp6p may take over the major role and process the 5.8S + 30 species to 6S pre-rRNA. In the absence of the exosome components some other activity is able to digest the 7S pre-rRNAs partially, producing the observed ladder of intermediates. This alternative activity is not provided by Rrp6p, since these species are detected in the *GAL::rrp41*/*rrp6*-Δ and *GAL::rrp45*/*rrp6*-Δ strains. Moreover, both the remaining exosome components and any alternative activity can poorly process the 5.8S + 30 pre-rRNAs since these accumulate to high levels in the *rrp6*-Δ strain. It is notable that the 3′ end of this species is predicted to lie in a stem structure, which may inhibit its processing if released as a free RNA. Unlike the larger intermediates that are specifically detected in the exosome mutants, the 6S pre-rRNAs are detected in the wild type. This may represent a site at which rapid processive processing is normally replaced by slower distributive trimming of the RNAs. The heterogeneity shown between different exosome mutant strains indicates that 6S pre-rRNA is processed by the exosome, rather than being the product of an alternative pathway that is activated in the absence of exosome activity. The pattern of intermediates observed during degradation of the 5′ ETS region of the pre-rRNA also

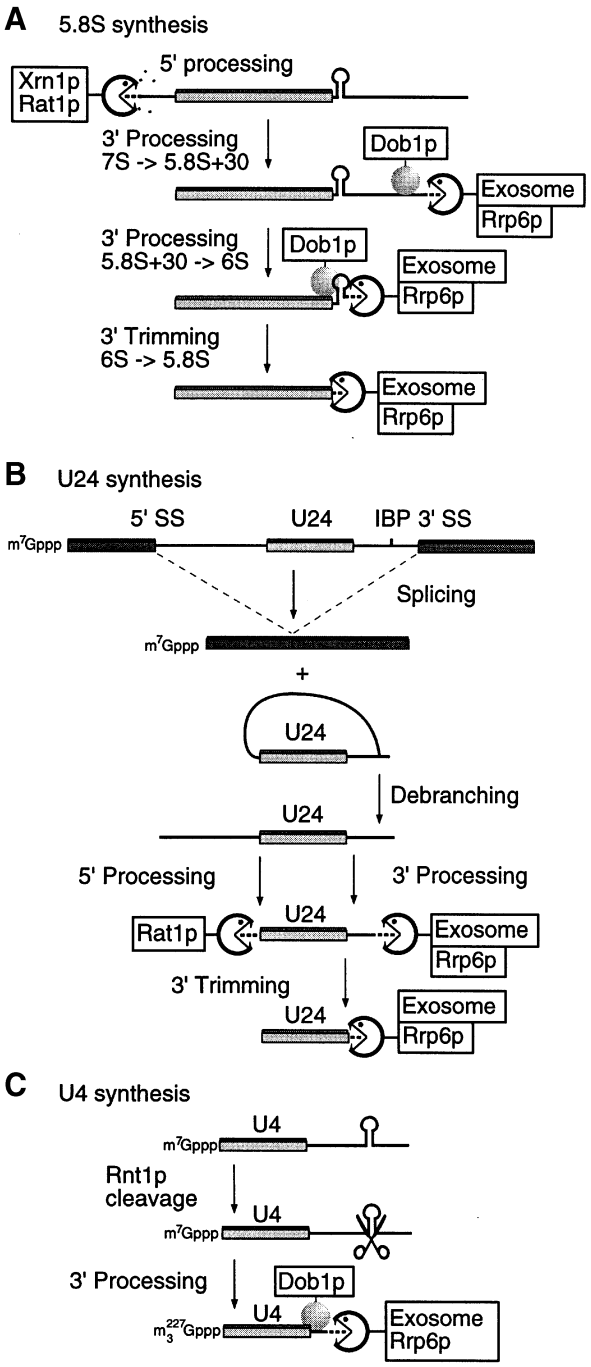

Fig. 9. Models for RNA processing pathways. (**A**) Processing of the 7S pre-rRNA to 5.8S rRNA. The mature rRNA is shown as a box and the transcribed spacers as lines. Processing of the 7S pre-rRNA to 5.8S + 30 requires all essential components of the exosome complex. Processing from 5.8S + 30 to 5.8S + 8 (6S pre-rRNA) specifically requires Rrp6p. The final trimming to the mature 5.8S again requires multiple exosome components. Each step requires the putative RNA helicase Dob1p/Mtr4p. 5.8S + 30 lies at the 3′ side of a predicted stem–loop structure. (**B**) Processing of the U24 snoRNA from the debranched intron lariat following mRNA splicing. The 5′ and 3′ exons are shown as dark boxes, the mature U24 is shown as a lighter box and the remainder of the intron as lines. (**C**) Processing of the U4 snRNA. An Rnt1p cleavage site lies in the 3′ flanking sequence and may act as an entry site for the exosome, acting together with Dob1p/Mtr4p. The timing of cap trimethylation of U4 is not clear. 3′ processing of snoRNAs and snRNAs is not blocked by mutation of individual components of the exosome indicating that other extrinsic or intrinsic activities can functionally replace these.

varies amongst the different exosome mutants, suggesting that exonuclease hand-over may be occurring during this processing.

Analysis of pre-snRNA processing reveals a complex picture. Each of the RNA polymerase II-transcribed snRNAs in yeast, U1, U2, U4 and U5, has a cleavage site for Rnt1p in the 3′ flanking region (Chanfreau *et al.*, 1997; Abou Elela and Ares, 1998; Seipelt *et al.*, 1999 and this work). For U1, U4 and U5 this may act as an entry site for the exosome complex, acting together with the Dob1p RNA helicase (see Figure 9C). However, in no case is synthesis of the snRNA blocked by the inhibition of cleavage by Rnt1p or by mutations in exosome components, indicating that alternative processing pathways exist.

In strains lacking Rnt1p the synthesis of long 3′ extended forms of U1 and U2 has been reported (Abou Elela and Ares, 1998; Seipelt *et al.*, 1999) and we show here that this is also the case for U4 and U5. During pre-rRNA processing, the 3′ end of the 35S pre-rRNA is normally cleaved cotranscriptionally by Rnt1p (Abou Elela *et al.*, 1996; Kufel *et al.*, 1999). In the absence of Rnt1p the pre-rRNA transcripts extend to a position close to the site of transcription termination. The extended U4 and U5 species form a ladder to a discrete size that we speculate represents the transcription termination site. These are not detected in the wild type, suggesting that pre-U4 and pre-U5 may also be cleaved cotranscriptionally. The extended species are substrates for the exosome since they accumulate at higher levels in *rnt1*-Δ strains that are depleted for exosome components. For both the pre-rRNA and U4, the excised 3′ fragments generated by Rnt1p cleavage are degraded by the 5′→3′ exonuclease Rat1p, which also processes the 5′ end of the $5.8S_s$ rRNA and many snoRNAs (see Figure 9B) (Amberg *et al.*, 1992; Henry *et al.*, 1994; Petfalski *et al.*, 1998; Villa *et al.*, 1998).

3′ maturation of snoRNAs that are excised from mRNA introns (U18 and U24) or from a dicistronic transcript (U14) also involves the exosome. U18 and U24 are predominately processed from the debranched intron lariat (Ooi *et al.*, 1998; Petfalski *et al.*, 1998; Villa *et al.*, 1998). In the exosome mutants we see accumulation of the species in which the 5′ end of the snoRNA has been matured but the intron is 3′ unprocessed (U18-3′ and U24-3′), together with a ladder that probably represents intermediates in the 3′ processing of these to the mature snoRNAs. The U18-3′ and U24-3′ RNAs also undergo some polyadenylation in strains lacking Rrp6p. In Rnt1p mutants, the 3′ extended forms of U1 and U2 that are generated also become polyadenylated (Abou Elela and Ares, 1998; Seipelt *et al.*, 1999), so this seems to be a general phenomenon in yeast. We conclude that 3′ processing of the debranched intron lariats containing U18 and U24 normally involves the exosome (see Figure 9B). Apparent intermediates in the 3′ processing of U14 are also observed, particularly in strains lacking both Rrp6p and Rrp41p. These may extend to the transcription termination site, but this has not yet been localized. Final trimming of each of these snoRNAs specifically requires Rrp6p. This activity apparently cannot be substituted by other exonucleases, since the entire snoRNA population is shifted in size by ~3 nt. This trimming activity is not clearly inhibited by mutations in other single components

Table II. Yeast strains used in this work

Strain	Genotype	Reference
BMA 38	*MAT***a**/α *ade2-1/ade2-1 his3-Δ200/his3-Δ200 leu2-3, 112/leu2-3, 112 trp1-1/trp1-1 ura3-1/ura3-1 can1-100/can1-100*	Baudin *et al.* (1993)
YCA12	*MAT***a** *ade2-1 his3-Δ200 leu2-3, 112 trp1-1 ura3-1 can1-100 RRP6::Kl TRP1*	Allmang *et al.* (1999)
YDL401	*MAT***a** *his3-Δ200 leu2-Δ1 trp1 ura3-52 gal2 galΔ108*	Lafontaine and Tollervey (1996)
P118	as YDL401 but *GAL10::prot.A-RRP41*	Lafontaine and Tollervey (1996)
YCA20	as YDL401 but *GAL10::RRP45*	Allmang *et al.* (1999)
YCA30	as YCA20 but *RRP6::Kl TRP1*	this study
YCA31	as P118 but *RRP6::Kl TRP1*	this study
YJK10	as YDL401 but *RNT1::TRP1*	this study
YJK11	as P118 but *RNT1::TRP1*	this study
YJK12	as YCA20 but *RNT1::TRP1*	this study
YJK13	as YCA12 but *RNT1::TRP1*	this study
GAL::DOB1	*MAT*α *ura3-1 ade2-1 his3-11,15 leu2-3, 112 trp1-1 dob1::HIS3MX6* + [pAS24-DOB1]	de la Cruz *et al.* (1998)
rat1-1	*MAT*α, *his3-Δ200, leu2-Δ1, ura3-52, rat1-1*	Amberg *et al.* (1992)
RP582	*MAT***a** *leu2-3, 112 ura3-52 rpb1-1*	Decker and Parker (1993)

of the exosome. It is notable that each of the enzymatic activities shown to be involved in pre-snoRNA processing, the exosome, the 5′→3′ exonuclease Rat1p and the endonuclease Rnt1p, also participate in pre-rRNA processing.

There are apparent similarities between 3′ processing of the 5.8S rRNA, snoRNAs and snRNAs. In each case there is a downstream cleavage, by endonuclease or splicing, which acts as a site of entry for exonucleases. Processing is at least biphasic with short 3′ extended forms accumulating, and each appears to involve the activities of more than one component of the exosome. In each case, other activities can partially substitute for the mutant exosome components. For the 7S pre-rRNA, and particularly the 5.8S + 30 pre-RNA, this is inefficient, and synthesis of mature 5.8S is strongly inhibited. The final trimming of snoRNAs is apparently completely dependent on the activity of Rrp6p, but the processing of further 3′ extended pre-snoRNAs and pre-snRNAs can be carried out by other activities with good efficiency, as shown by the wild-type levels of the mature RNAs. Indeed, U4, and particularly $U5_S$, are synthesized at substantially elevated levels in exosome mutants, indicating competition between synthesis of mature snRNA and degradation of the precursors in the wild type.

It is unclear whether residual processing in the exosome mutant strains is carried out by other components of the complex. It is notable that double-mutant strains lacking both Rrp6p and Rrp41p show stronger phenotypes for some activities (e.g. 3′ processing of U14 and U18) than does either single mutant, indicating that the absence of one component does not necessarily inactivate the entire complex. Alternatively, the yeast genome contains several other predicted 3′→5′ exonucleases (Mian, 1997; Moser *et al.*, 1997) that may be able to partially substitute for the exosome. The combination of mutations in these genes with mutations in exosome components will now be needed to analyse their interactions and substrates.

Materials and methods

Strains

Growth and handling of *S.cerevisiae* were by standard techniques. The transformation procedure was according to Gietz *et al.* (1992). Except where stated, strains were grown in liquid and solid minimal medium containing 0.67% yeast nitrogen base (Difco) and 2% glucose. *GAL*-regulated strains were pre-grown in RSG medium (2% raffinose, 2% sucrose, 2% galactose, 0.67% yeast nitrogen base) and harvested at intervals following a shift to 2% glucose.

Yeast strains used and constructed in this study are listed in Table II.

To construct the double mutants *GAL10::rrp45*/*rrp6*-Δ (YCA30) and *GAL10::rrp41*/*rrp6*-Δ (YCA31), the *RRP6::TRP* disrupted allele was amplified by PCR from genomic DNA extracted from *rrp6*-Δ (YCA12). The PCR product was transformed into the corresponding conditional mutant strains P118 and YCA20, respectively. The amplification of *RRP6::TRP* was done with oligos: 5′RRP6, CAGTAATGAATATTAATGTTCATCTGAAGATAGACG; 3′RRP6, ATGGTGTGCATGGGGGAGCCATAACTCCATGACACA. Strains YDL401, P118 and YCA20 were used to construct the mutants *rnt1*-Δ (YJK10), *GAL10::rrp41*/*rnt1*-Δ (YJK11) and *GAL10::rrp45*/*rnt1*-Δ (YJK12), using the same PCR strategy. Oligonucleotides 5′RNT1, 5′-GAAGACATATCCGAAGTGACA and 3′RNT1, 5′-GGATTTCTATACCCTCGAGGAG, complementary to sequences beyond the *RNT1* gene, were used for the amplification with genomic DNA extracted from *rnt1*-Δ strain generously provided by G.Chanfreau (Chanfreau *et al.*, 1998b). Transformants were selected for Trp^+ prototrophy and were screened by PCR. The phenotypes of respective constructs were confirmed by Northern hybridization. Strain *rrp6*-Δ/*rnt1*-Δ (YJK13) was constructed by crossing YJK10 and YCA12 strains. The double-mutant strain was selected from dissected full tetrads by testing for the pre-rRNA and snoRNA processing phenotypes by Northern hybridization. Wild-type *RNT1* and *rnt1*-Δ sister strains (Chanfreau *et al.*, 1998b) were used to prepare whole-cell extract. Strain *rat1-1* was kindly provided by C.Cole (Amberg *et al.*, 1992).

RNA extraction, Northern hybridization and primer extension

RNA was extracted as described previously (Tollervey and Mattaj, 1987). Northern hybridization (Tollervey, 1987) and primer extension (Beltrame and Tollervey, 1992) were as described previously. Standard 6 or 8% acrylamide gels were used to analyse low molecular weight rRNA species and primer extension reactions.

For pre-rRNA and rRNA analysis the following oligonucleotides were used: 017 5′-GCGTTGTTCATCGATGC; 020 5′-TGAGAAGGAAATGACGCT; 033 5′-CGCTGCTCACCAATGG; 041 5′-CTACTCGGTCAGGCTC.

The oligonucleotides used for Northern blot hybridization and primer extensions on other small RNAs were as follows: 031 (MRP) 5′-AATAGAGGTACCAGGTCAAGAAGC; 201 (snR190) 5′-CGTCATGGTCGAATCGG; 202 (U14) 5′-TCACTCAGACATCCTAGG; 205 (U18) 5′-GTCAGATACTGTGATAGTC; 206 (U18-3′) 5′-GCTCTGTGTGCTATCGTC; 210 (U14-3′) 5′-GTATACGATCACTCAGAC; 213 (U24-3′) 5′-AAACCATTCATCAGAG; 214 (U24) 5′-TCAGAGATCTTGGTGATAAT; 218 (snR10, 2′-*O*-methyl RNA) 5′-CUIUUAAAUUUICIUU; 236 (snR39) 5′-GGTGATAAGTTACGACAGC; 238 (snR41) 5′-GGGTTGTCGACATGTAGTTA; 242 (U1) 5′-CACGCCTTCCGCGCCGT; 243 (U4) 5′-CCGTGCATAAGGAT; 244 (U5) 5′-AATATGGCAAGCCC; 245 (3′Ex-U1) 5′-TGTTCCATTTATTTCTGAAA; 246 (3′Ex-U4) 5′-AAAGAATGAATATCGGTAATG; 247 ($3'Ex\text{-}U5_S$) 5′-GAGAAAAAGGGCAGAAAAG; 248 ($3'Ex\text{-}U5_L$) 5′-TAGAAAAGATAAACGCCCT; 249 (U4DS) 5′-GACACACAAGAAGGAGAACACTC; 250 (SCR1) 5′-AAGGACCCAGAACTACCTTG.

RNase H treatment

Deadenylation was performed essentially as described (Decker and Parker, 1993). Samples of 30 µg of RNA were annealed with 750 ng oligo(dT) at 65°C for 1 h and digested with 6 U RNase H at 30°C for 1 h. The control samples were treated identically, except that the oligo(dT) was omitted.

In vitro processing reactions

Synthetic U4-3′ RNA was obtained by *in vitro* transcription as described (Chanfreau *et al.*, 1998b) using PCR product as template. PCR product was generated from genomic DNA using a forward primer carrying a T7 promoter (T7U4DS, 5′-GCGAATTCTAATACGACTCACTATAGG-AAGTAATATCAAAAAATAGG) and a reverse primer U4DS.

Whole-cell extracts were prepared from wild-type and *rnt1*Δ sister strains as described (Chanfreau *et al.*, 1998b).

Recombinant His_6–Rnt1p was prepared by cloning a PCR-amplified *RNT1* gene into pET16B (Novagen), using *Nde*I and *Bam*HI restriction sites added into the primers (*Nde*I–*Rnt*I, 5′-GGGAATTCCATATGGGCT-CAAAAGTAGCAGG; *Bam*–*Rnt*I, 3′-CGGGATCCTCAGCTTGTAT-CTGAGAATTTTCTTTTCTTATTC). Expression of His_6–Rnt1p in *E.coli* strain BL21 was induced by addition of isopropyl-β-D-galactopyranoside at $OD_{0.5}$ (final concentration 0.5 mM). After 3 h of expression at 30°C, cells were harvested and pellets were kept at –80°C. Pellets were resuspended in 40 ml of Start buffer (20 mM sodium phosphate pH 7.0, 10 mM imidazole) and cells were further lysed by passing through a French press. Cell debris were pelleted and the supernatant was loaded into a Hi-Trap Chelating column (Pharmacia) pre-equilibrated with the Start buffer. The column was washed with 10 ml Start buffer and proteins were eluted with sodium phosphate buffer with increasing imidazole concentration (20, 40, 60, 100, 300 and 500 mM) or a linear gradient of imidazole (10–500 mM). Peak fractions were pooled and the protein was dialysed twice against the storage buffer (50% glycerol, 50 mM Tris–HCl pH 7.6, 200 mM KCl, 0.5 mM dithiothreitol, 0.5 mM EDTA pH 8.5). The protein was stored at a concentration of 2 mg/ml at –20°C and remained active for several months after storage.

In vitro processing of U4-3′ RNA in cell extracts or with recombinant His_6–Rnt1p, and mapping of the cleavage sites using primer extension, was performed as described (Chanfreau *et al.*, 1998a,b). Prior to the reaction, gel-purified RNA substrates (2 nM) were denatured for 2 min at 85°C in the Rnt1p buffer (50 mM Tris–HCl pH 7.6, 200 mM KCl, 0.1 mg/ml wheat-germ tRNA, 5 mM $MgCl_2$) and cooled to 23°C. The cleavage reaction was performed either at 23°C using from 50 to 200 fmol of recombinant His_6–Rnt1 or by incubation in the whole-cell extracts.

Acknowledgements

J.K. was the recipient of a long-term EMBO fellowship. This work was supported by the Wellcome Trust.

References

Abou Elela,S. and Ares,M.,Jr (1998) Depletion of yeast RNase III blocks correct U2 3′ end formation and results in polyadenylated but functional U2 snRNA. *EMBO J.*, **17**, 3738–3746.

Abou Elela,S., Igel,H. and Ares,M.,Jr (1996) RNase III cleaves eukaryotic preribosomal RNA at a U3 snoRNP-dependent site. *Cell*, **85**, 115–124.

Allmang,C., Petfalski,E., Podtelejnikov,A., Mann,M., Tollervey,D. and Mitchell,P. (1999) The yeast exosome and human PM-Scl are related complexes of 3′→5′ exonucleases. *Genes Dev.*, **13**, 2148–2158.

Amberg,D.C., Goldstein,A.L. and Cole,C.N. (1992) Isolation and characterization of *RAT1*: an essential gene of *Saccharomyces cerevisiae* required for the efficient nucleocytoplasmic trafficking of mRNA. *Genes Dev.*, **6**, 1173–1189.

Baker,R.E., Harris,K. and Zhang,K. (1998) Mutations synthetically lethal with *cep1* target *S.cerevisiae* kinetochore components. *Genetics*, **149**, 73–85.

Baudin,A., Ozier-Kalogeropoulos,O., Denouel,A., Lacroute,F. and Cullin,C. (1993) A simple and efficient method for direct gene deletion in *Saccharomyces cerevisiae*. *Nucleic Acids Res.*, **21**, 3329–3330.

Beltrame,M. and Tollervey,D. (1992) Identification and functional analysis of two U3 binding sites on yeast pre-ribosomal RNA. *EMBO J.*, **11**, 1531–1542.

Briggs,M.W., Burkard,K.T. and Butler,J.S. (1998) Rrp6p, the yeast homologue of the human PM-Scl 100-kDa autoantigen, is essential for efficient 5.8 S rRNA 3′ end formation. *J. Biol. Chem.*, **273**, 13255–13263.

Caffarelli,E., Arese,M., Santoro,B., Fragapane,P. and Bozzoni,I. (1994) *In vitro* study of processing of the intron-encoded U16 small nucleolar RNA in *Xenopus laevis*. *Mol. Cell. Biol.*, **14**, 2966–2974.

Caffarelli,E., De Gregorio,E., Fatica,A., Prislei,S., Fragapane,P. and Bozzoni,I. (1996) Processing of the intron-encoded U16 and U18 snoRNAs: the conserved C and D boxes control both the processing reactions and the stability of the mature snoRNAs. *EMBO J.*, **15**, 1121–1131.

Cavaillé,J. and Bachellerie,J.-P. (1996) Processing of fibrillarin-associated snoRNAs from pre-mRNA introns: an exonucleolytic process exclusively directed by the common stem-box terminal structure. *Biochimie*, **78**, 443–456.

Cecconi,F., Mariottini,P. and Amaldi,F. (1995) The *Xenopus* intron-encoded U17 snoRNA is produced by exonucleolytic processing of its precursor in oocytes. *Nucleic Acids Res.*, **23**, 4670–4676.

Chanfreau,G., Elela,S.A., Ares,M.,Jr and Guthrie,C. (1997) Alternative 3′-end processing of U5 snRNA by RNase III. *Genes Dev.*, **11**, 2741–2751.

Chanfreau,G., Legrain,P. and Jacquier,A. (1998a) Yeast RNase III as a key processing enzyme in small nucleolar RNAs metabolism. *J. Mol. Biol.*, **284**, 975–988.

Chanfreau,G., Rotondo,G., Legrain,P. and Jacquier,A. (1998b) Processing of a dicistronic small nucleolar RNA precursor by the RNA endonuclease Rnt1. *EMBO J.*, **17**, 3726–3737.

de la Cruz,J., Kressler,D., Tollervey,D. and Linder,P. (1998) Dob1p (Mtr4p) is a putative ATP-dependent RNA helicase required for the 3′ end formation of 5.8S rRNA in *Saccharomyces cerevisiae*. *EMBO J.*, **17**, 1128–1140.

Decker,C.J. and Parker,R. (1993) A turnover pathway for both stable and unstable mRNAs in yeast: evidence for a requirement for deadenylation. *Genes Dev.*, **7**, 1632–1643.

Gietz,D., St Jean,A., Woods,R.A. and Schiestl,R.H. (1992) Improved method for high efficiency transformation of intact yeast cells. *Nucleic Acids Res.*, **20**, 1425.

Henry,Y., Wood,H., Morrissey,J.P., Petfalski,E., Kearsey,S. and Tollervey,D. (1994) The 5′ end of yeast 5.8S rRNA is generated by exonucleases from an upstream cleavage site. *EMBO J.*, **13**, 2452–2463.

Kenna,M., Stevens,A., McCammon,M. and Douglas,M.G. (1993) An essential yeast gene with homology to the exonuclease-encoding *XRN1*/*KEM1* gene also encodes a protein with exoribonuclease activity. *Mol. Cell. Biol.*, **13**, 341–350.

Kiss,T., Bortolini,M.-L. and Filipowicz,W. (1996) Characterization of the intron-encoded U19 RNA, a new mammalian small nucleolar RNA that is not associated with fibrillarin. *Mol. Cell. Biol.*, **16**, 1391–1400.

Kiss-László,Z., Henry,Y., Bachellerie,J.-P., Caizergues-Ferrer,M. and Kiss,T. (1996) Site-specific ribose methylation of preribosomal RNA: a novel function for small nucleolar RNAs. *Cell*, **85**, 1077–1088.

Kretzner,L., Rymond,B.C. and Rosbash,M. (1987) *S.cerevisiae* U1 RNA is large and has limited primary sequence homology to metazoan U1 snRNA. *Cell*, **50**, 593–602.

Kufel,J., Dichtl,B. and Tollervey,D. (1999) Yeast Rnt1p is required for cleavage of the pre-ribosomal RNA in the 3′ ETS but not the 5′ ETS. *RNA*, **5**, 909–917.

Lafontaine,D. and Tollervey,D. (1996) One-step PCR mediated strategy for the construction of conditionally expressed and epitope tagged yeast proteins. *Nucleic Acids Res.*, **24**, 3469–3472.

Larimer,F.W., Hsu,C.L., Maupin,M.K. and Stevens,A. (1992) Characterization of the *XRN1* gene encoding a 5′→3′ exoribonuclease: sequence data and analysis of disparate protein and mRNA levels of gene-disrupted yeast cells. *Gene*, **120**, 51–57.

Li,Z., Pandit,S. and Deutscher,M.P. (1998) 3′ exoribonucleolytic trimming is a common feature of the maturation of small, stable RNAs in *Escherichia coli*. *Proc. Natl Acad. Sci. USA*, **95**, 2856–2861.

Maxwell,E.S. and Fournier,M.J. (1995) The small nucleolar RNAs. *Annu. Rev. Biochem.*, **35**, 897–934.

Mian,I.S. (1997) Comparative sequence analysis of ribonucleases HII, III, II PH and D. *Nucleic Acids Res.*, **25**, 3187–3195.

Mitchell,P., Petfalski,E. and Tollervey,D. (1996) The 3′-end of yeast 5.8S rRNA is generated by an exonuclease processing mechanism. *Genes Dev.*, **10**, 502–513.

Mitchell,P., Petfalski,E., Shevchenko,A., Mann,M. and Tollervey,D. (1997) The exosome; a conserved eukaryotic RNA processing complex

containing multiple 3′→5′ exoribonuclease activities. *Cell*, **91**, 457–466.
Moser,M.J., Holley,W.R., Chatterjee,A. and Mian,I.S. (1997) The proofreading domain of *Escherichia coli* DNA polymerase I and other DNA and/or RNA exonuclease domains. *Nucleic Acids Res.*, **25**, 5110–5118.
Noguchi,E. *et al.* (1996) Dis3, implicated in mitotic control, binds directly to Ran and enhances the GEF activity of RCC1. *EMBO J.*, **15**, 5595–5605.
Ooi,S.L., Samarsky,D.A., Fournier,M.J. and Boeke,J.D. (1998) Intronic snoRNA biosynthesis in *Saccharomyces cerevisiae* depends on the lariat-debranching enzyme: intron length effects and activity of a precursor snoRNA. *RNA*, **4**, 1096–1110.
Patterson,B. and Guthrie,C. (1987) An essential yeast snRNA with a U5-like domain is required for splicing *in vivo*. *Cell*, **49**, 613–624.
Petfalski,E., Dandekar,T., Henry,Y. and Tollervey,D. (1998) Processing of the precursors to small nucleolar RNAs and rRNAs requires common components. *Mol. Cell. Biol.*, **18**, 1181–1189.
Qu,L.H., Henry,Y., Nicoloso,M., Michot,B., Azum,M.C., Renalier,M.H., Caizergues-Ferrer,M. and Bachellerie,J.P. (1995) U24, a novel intron-encoded small nucleolar RNA with two 12 nt long, phylogenetically conserved complementarities to 28S rRNA. *Nucleic Acids Res.*, **23**, 2669–2676.
Qu,L.H. *et al.* (1999) Seven novel methylation guide small nucleolar RNAs are processed from a common polycistronic transcript by Rat1p and RNase III in yeast. *Mol. Cell. Biol.*, **19**, 1144–1158.
Seipelt,R.L., Zheng,B., Asuru,A. and Rymond,B.C. (1999) U1 snRNA is cleaved by RNase III and processed through an Sm site-dependent pathway. *Nucleic Acids Res.*, **27**, 587–595.
Siliciano,P.G., Jones,M.H. and Guthrie,C. (1987) *Saccharomyces cerevisiae* has a U1-like small nuclear RNA with unexpected properties. *Science*, **237**, 1484–1487.
Tollervey,D. (1987) A yeast small nuclear RNA is required for normal processing of pre-ribosomal RNA. *EMBO J.*, **6**, 4169–4175.
Tollervey,D. and Mattaj,I.W. (1987) Fungal small nuclear ribonucleoproteins share properties with plant and vertebrate U-snRNPs. *EMBO J.*, **6**, 469–476.
Veldman,G.M., Klootwijk,J., van Heerihuizen,H. and Planta,R.J. (1981) The nucleotide sequence of the intergenic region between the 5.8S and 26S rRNA genes of the yeast ribosomal RNA operon. Possible implications for the interaction between 5.8S and 26S rRNA and the processing of the primary transcript. *Nucleic Acids Res.*, **9**, 4847–4862.
Villa,T., Ceradini,F., Presutti,C. and Bozzoni,I. (1998) Processing of the intron-encoded U18 small nucleolar RNA in the yeast *Saccharomyces cerevisiae* relies on both exo- and endonucleolytic activities. *Mol. Cell. Biol.*, **18**, 3376–3383.
Yeh,L.C. and Lee,J.C. (1990) Structural analysis of the internal transcribed spacer 2 of the precursor ribosomal RNA from *Saccharomyces cerevisiae*. *J. Mol. Biol.*, **211**, 699–712.
Yoo,C.J. and Wolin,S.L. (1997) The yeast La protein is required for the 3′ endonucleolytic cleavage that matures tRNA precursors. *Cell*, **89**, 393–402.
Zagorski,J., Tollervey,D. and Fournier,M.J. (1988) Characterization of an *SNR* gene locus in *Saccharomyces cerevisiae* that specifies both dispensable and essential small nuclear RNAs. *Mol. Cell. Biol.*, **8**, 3282–3290.

Received June 24, 1999; revised and accepted August 10, 1999